Codimension-two singularities on the stability boundary in 2D Filippov systems

F. Dercole [*] **F. Della Rossa** [*,**] **A. Colombo** [***]
Yu. A. Kuznetsov [****]

[*] *Dipartimento di Elettronica e Informazione, Politecnico di Milano,*
Via Ponzio 34/5, 20133 Milan, Italy
(e-mail: {fabio.dercole@,fabio.dellarossa@mail.}polimi.it)
[**] *MRI Masterclass participant at Department of Mathematics,*
Utrecht University, Utrecht, The Netherlands
[***] *Department of Mechanical Engineering, Massachusetts Institute of*
Technology, 77 Massachusetts Avenue, Cambridge, Massachusetts
02139, USA (e-mail: acolombo@mit.edu)
[****] *Department of Mathematics, Utrecht University, Budapestlaan 6,*
3584 CD Utrecht, The Netherlands (e-mail: I.A.Kouznetsov@uu.nl)

Abstract: Bifurcation theory provides powerful tools for the analysis of the dynamics of open-loop or closed-loop nonlinear control systems. These systems are Filippov (or piecewise smooth) when the dynamics depends discontinuously on the state, for example as a consequence relay feedback actions. In this paper we contribute to the analysis of codimension-two bifurcations in Filippov systems by reporting some results on the equilibrium bifurcations of 2D systems that involve a sliding limit cycle. There are only two such local bifurcations: a degenerate boundary focus that we call *homoclinic boundary focus*; and the *boundary Hopf*. We address both of them, and provide the complete set of curves that exist around such codimension-two bifurcation points. Existing numerical software can be used to exploit these results for the analysis of the stability boundaries of nonlinear piecewise smooth control systems. In the final part of this paper, we discuss a 2D Filippov system modelling an ecosystem subject to on-off harvesting control that exhibits both codimension-two bifurcations.

Keywords: Nonlinear system, Nonlinear control, Piecewise smooth, Sliding, Stability domains, Relay control, Ecology.

1. INTRODUCTION

With the help of many publicly available numerical packages (e.g., Doedel et al. (2007); Dhooge et al. (2002); Kuznetsov and Levitin (1997)) the boundaries of stability of the asymptotic solutions of a nonlinear control system can be reconstructed as the parameters are changed, and the solutions can be followed as their stability and topological structure change with the system's parameters (Kuznetsov, 2004; Krener et al., 2004; Astolfi and Marconi, 2008). This proves an especially valuable tool when dealing with multistable systems, where the coexistence of multiple attractors renders the analysis by simulation ineffective. It represents also, quite often, a uniquely effective way to prove the existence of periodic and quasiperiodic solutions, by detecting their onset, for example, at Hopf and torus (Neimak-Sacker) bifurcations. Finally, knowledge of the dynamic transitions of solutions through bifurcations is being exploited to accomplish control-based continuation of solutions beyond their domains of stability, both in virtual and in experimental setups (Sieber et al., 2008, 2009), providing ways to test the dynamic behaviour of nonlinear structures beyond their breaking point.

In all these applications, though the algebraic conditions for the detection of a bifurcation are a necessary ingredi-

ent, useful results are obtained only with the knowledge of the dynamics expected near the bifurcating solution. The description of all invariant sets (equilibria, cycles, etc.) that must exist near a bifurcating solution is known, in the mathematical jargon, as the bifurcation's *unfolding*.

In the study of a system's bifurcation diagram, a special role is played by *codimension-two* bifurcations, which appear in a two-parameter diagram as points of intersection of several bifurcation curves. Their unfolding must describe not only the dynamics nearby, but also all the bifurcation curves (called *codimension-one* bifurcations) that are rooted at such points. Knowledge of these unfoldings thus provides a simple way to deduce the presence of a number of bifurcation curves, once a codimension-two point has been detected. A classic example is the famous Bogdanov-Takens bifurcation (see, e.g., Kuznetsov (2004)), where the presence of a codimension-two equilibrium with a double zero eigenvalue implies the existence of a Hopf, a saddle node, and a homoclinic bifurcation curves.

In the case of smooth systems, both in discrete and continuous time, the unfoldings of all the most common codimension-one and -two bifurcations are well known. In nonsmooth systems however, new bifurcations are found, that involve the interaction of invariant sets with the

system's discontinuity boundaries. These are commonly called *discontinuity-induced* bifurcations (di Bernardo et al., 2008a). The theory of nonsmooth systems is at a much more primitive stage than its smooth counterpart, and though some progresses have been made in unfolding codimension-one and -two discontinuity induced bifurcations, an adequate understanding of these systems lies still quite distant (Colombo et al., submitted). An interesting exception is given by planar *Filippov* systems.

A Filippov (or piecewise smooth) system (Filippov, 1988) is composed of different smooth ODEs defined in open non-intersecting domains S_i, separated by smooth *discontinuity boundaries*. In the simplest case of two adjacent parameter-dependent domains $S_{1,2} \in \mathbb{R}^n$:

$$S_1(\alpha) = \{x \in \mathbb{R}^n : H(x, \alpha) < 0\},$$
$$S_2(\alpha) = \{x \in \mathbb{R}^n : H(x, \alpha) > 0\},$$

$\alpha \in \mathbb{R}^m$, separated by a smooth $(n-1)$-dimensional boundary $\Sigma(\alpha) = \{x \in \mathbb{R}^n : H(x, \alpha) = 0\}$, where H is a smooth scalar function with nonvanishing gradient $H_x(x, \alpha)$ on Σ, a Filippov system is defined as

$$\dot{x} = \begin{cases} f^{(1)}(x, \alpha), & x \in S_1(\alpha), \\ f^{(2)}(x, \alpha), & x \in S_2(\alpha). \end{cases} \quad (1)$$

Here $f^{(1,2)}$ are smooth parameter-dependent vector fields, and the dot stands for time-derivative w.r.t. time.

Orbits cross Σ at points where the components of $f^{(1,2)}$ orthogonal to Σ (i.e., those along $H_x(x, \alpha)$) have the same direction. Where these components have opposite directions, the system admits a solution that slides on Σ in accordance with the *Filippov vector field*:

$$\dot{x} = (1 - \lambda)f^{(1)}(x, \alpha) + \lambda f^{(2)}(x, \alpha), \quad (2)$$

λ being selected so that $\dot{x}$ is tangent to Σ. Sliding is stable (and simply called *sliding*) when Σ is attracting ($f^{(1,2)}$ push toward Σ) and unstable (called *escaping*) in the opposite case.

The $(n-2)$-dimensional borders between the crossing and sliding regions of Σ are generically composed of *tangency points*, where one of the vector fields $f^{(1,2)}$ is tangent to Σ ($\lambda = 0, 1$ in (2)). As shown in Fig. 1, a tangency point of $f^{(i)}$ is called *visible* if the orbit of $f^{(i)}$ passing through the point is locally defined in S_i, it is called *invisible* otherwise.

Generic equilibria of (1) can be standard equilibria of $f^{(1,2)}$ in $S_{1,2}$ or equilibria of the Filippov vector field with $\lambda \in (0, 1)$, called *pseudoequilibria*, where $f^{(1,2)}$ are nonzero and anticollinear. The stability of pseudoequilibria is determined by the Filippov vector field together with the stability of the sliding. Pseudoequilibria are reached in finite time along a direction transverse to Σ. Standard equilibria and pseudoequilibria of (1) are called *admissible*, while equilibria of $f^{(i)}$ in S_j, $i \neq j$, and equilibria of (2) in the crossing region ($\lambda < 0$ or $\lambda > 1$) are called *virtual*.

Fig. 1. Orbits in a region S_i of the state space, with tangency points marked by black dots. Left/Right: a visible/invisible tangency point of the vector field.

The complete unfolding of most codimension-one discontinuity induced bifurcations of planar Filippov systems has been presented in Kuznetsov et al. (2003), together with canonical one-parameter bifurcation diagrams, but a way to generalize the results to arbitrary dimensions is still unknown.

In this paper, we contribute to the analysis of codimension-two bifurcations in discontinuous systems by studying all equilibrium (local) bifurcations in 2D Filippov systems that involve codimension-one bifurcations of sliding limit cycles. It follows from the visual inspection of all codimension-one cases treated in Kuznetsov et al. (2003) that such codimension-two bifurcations can only occur at a degenerate *boundary focus* (BF, a focus equilibrium of vector fields $f^{(1)}$ or $f^{(2)}$ colliding with the discontinuity boundary). There are actually only two cases. In one case the focus collides with a visible tangency point and a pseudo-saddle and, at the same time, the infinitesimal loop originated at the tangency point merges with the stable manifold of the pseudo-saddle. As a result, a small *sliding homoclinic orbit to pseudo-saddle* exists close to the codimension-two bifurcation and the corresponding codimension-one bifurcation curve emanates from the codimension-two point in the universal local bifurcation diagram. For this reason, we call this codimension-two bifurcation *homoclinic boundary focus* (HBF). The second degenerate boundary focus is the *boundary Hopf* (BH) at which the focus collides with the discontinuity boundary while being at the same time nonhyperbolic. The small-amplitude limit cycle originating through the Hopf bifurcation grazes the discontinuity boundary close to the codimension-two bifurcation, so that a codimension-one grazing bifurcation curve emanates from the codimension-two point at the BH bifurcation.

In what follows, we provide the unfoldings of these two bifurcations, and briefly sketch the analytical steps to obtain them. The complete analysis will be reported in Dercole et al. (submitted). In both cases, starting from a generic 2D Filippov system showing the bifurcation, we derive a canonical form to which the system can be reduced through explicit changes of variables and parameters (and time reparametrization in the BH case), locally to the codimension-two point in a two-parameter space. The bifurcation analysis is then performed on the canonical forms and provides explicit genericity conditions expressed in the original variables and parameters. While the unfolding of the HBF case is new and rather involved, the BH case is easier and already addressed in di Bernardo et al. (2008b) and Guardia et al. (2009). However, as precisely discussed in Sect. 3, the system analysed in the first reference is not fully generic, whereas the approach followed in the second does not provide a means to compute the genericity conditions numerically.

2. HOMOCLINIC BOUNDARY FOCUS

The first codimension-two bifurcation that we study—HBF—occurs at the border between the two codimension-one BF bifurcations named BF_1 and BF_2 in Fig. 2. We consider a planar system defined as in (1), where $f^{(1)}$ has a focus in $x = 0$, while $\alpha \in \mathbb{R}^2$, $\alpha = 0$ being the codimension-two point. Furthermore, we assume the
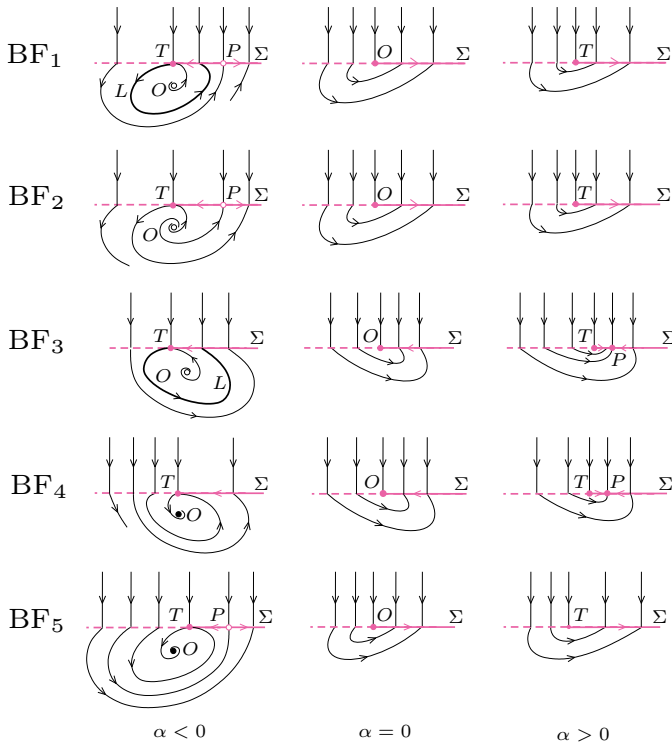
Fig. 2. The unfoldings of the five BF bifurcations discussed in Kuznetsov et al. (2003). T, tangency point; P, pseudoequilibrium; O, focus; L, sliding cycle. Bifurcations BF_1, BF_2, and BF_5 are said to be *nonsmooth fold* scenarios (di Bernardo et al., 2008a), since they imply the collision and annihilation of an equilibrium (O) and a pseudoequilibrium (P), while bifurcations BF_3 and BF_4 are called *persistence* scenarios, as a stationary solution persists through the bifurcation.

following conditions:

(G.1) $(f^{(1)})^0 = 0$, $H^0 = 0$, $\lambda_{1,2}^0 = \mu^0 \pm i\omega^0$, $\mu^0, \omega^0 > 0$,
(G.2) $H_x^0 (f^{(2)})^0 \neq 0$,
(G.3) $H_\alpha^0 \neq 0$,
(G.4) $H_x^0 ((f_x^{(1)})^0)^{-1} (f^{(2)})^0 < 0$,
(G.5) the system changes from BF_1 to BF_2 at $\alpha = 0$,

where the 0-superscript stands for evaluation at $(x, \alpha) = (0, 0)$, $f_x^{(1)}$ is the gradient of $f^{(1)}$, and $\lambda_{1,2}^0$ are the eigenvalues of $(f_x^{(1)})^0$. Conditions (G.1)–(G.4) require that $x = 0$ is an unstable focus (the stable case can be obtained by reversing the direction of time and thus involves escaping instead of sliding) and that no other degeneracy but (G.5) occurs at $\alpha = 0$. In particular, negativity of the left-hand side of (G.4) ensures a nonsmooth fold BF scenario, as defined in the caption of Fig. 2.

Under these conditions, through an invertible change of coordinates and parameters (detailed in Dercole et al. (submitted)) that leaves the focus in the origin, the system can be put in the form

$$\dot{z} = \begin{cases} f(z, \beta), & z_2 < \beta_1, \\ [0, -1]^\top, & z_2 > \beta_1, \end{cases} \tag{3}$$

where the boundary Σ is horizontal, region S_1 is below the boundary, and the vector field in S_2 is constant and vertically points downward. The parameter β_1 is the

distance of the equilibrium $z = 0$ from Σ, hence the BF bifurcation curve has equation $\beta_1 = 0$ (the β_2-axis), with the equilibrium $z = 0$ admissible for $\beta_1 > 0$ and virtual for $\beta_1 < 0$. The parameter β_2 can be chosen so that it is positive in the scenario BF_1, negative in BF_2, and equal to 0 at the codimension-two bifurcation (an explicit test-function $\beta_2 = \varphi(\alpha)$ to detect the codimension-two point along the BF curve is described in Dercole et al. (submitted), so that (G.5) becomes $\langle \varphi_\alpha^0, (H_\alpha^\perp)^0 \rangle \neq 0$, where $H_\alpha^\perp = [H_{\alpha_2}, -H_{\alpha_1}]$ is tangent to the BF curve).

Inspecting the portraits in Fig. 2 it is easy to see that, at the BF_1–BF_2 transition (see left panels), the orbit departing from the tangency point reaches the discontinuity boundary vertically, thus generating a sliding homoclinic cycle (a homoclinic cycle to a pseudoequilibrium). This can be proved rigorously by studying the asymptotic expansion of this orbit. The linear expansion of the SH curve takes the form

$$\tfrac{1}{2} s_{20} \beta_1 + s_{11} \beta_2 = 0, \tag{4}$$

where the coefficient $s_{11} \neq 0$ provided (G.4) and (G.5) (see Dercole et al. (submitted)). A trivial parameter change makes the SH bifurcation locally correspond to the positive β_1-axis.

Close to $\beta = 0$ there are generically (i.e., under conditions (G.1)–(G.5)) no other bifurcations. In fact, the equilibrium $z = 0$ remains hyperbolic and the boundary-equilibrium scenario (nonsmooth-fold) does not change for small $\|\beta\|$. Thus, there is a unique equilibrium ($z = 0$) and a unique pseudoequilibrium (P) involved in the HBF bifurcation, and the only possible global bifurcation is the SH bifurcation that we have discussed. The bifurcation diagram of the HBF singularity locally to $\beta = 0$ is hence that of Fig. 3, where the positive/negative β_2-axis is the BF_1/BF_2 BF branch, while the positive β_1-axis correspond to the SH bifurcation. The labelling of the corresponding state portraits is in accordance with Fig. 2.
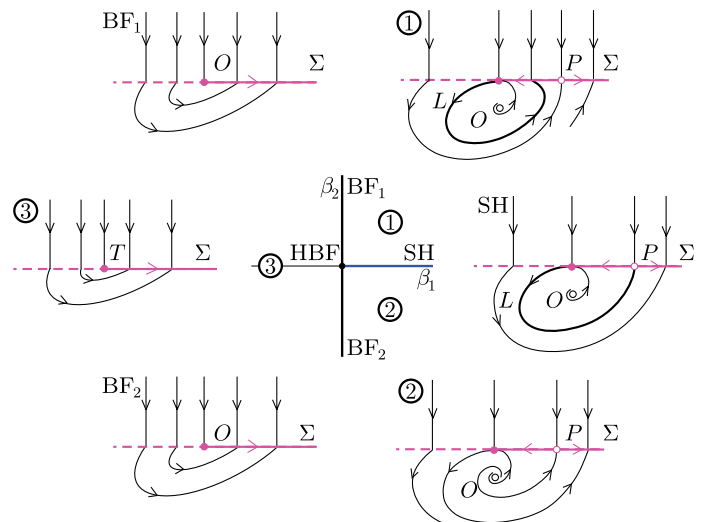

Fig. 3. HBF universal local bifurcation diagram. The BF curves are in blue, the sliding homoclinic in red.

3. BOUNDARY HOPF

The second codimension-two bifurcation that we consider—BH—occurs when a focus on the discontinuity boundary Σ has purely imaginary eigenvalues. Generically, this implies that the focus undergoes a (Andronov-)Hopf bifurcation.

As in the previous section, $\alpha \in \mathbb{R}^2$, and $\alpha = 0$ is the codimension-two point. We assume the following conditions:

(G.1) $(f^{(1)})^0 = 0$, $H^0 = 0$, $\lambda_{1,2}^0 = \pm i\omega^0 \neq 0$,

(G.2) $H_x^0 (f^{(2)})^0 \neq 0$,

(G.3) $H_\alpha^0 \neq 0$,

(G.4) $H_x^0 ((f_x^{(1)})^0)^{-1}(f^{(2)})^0 \neq 0$,

where (G.2) and (G.3) are the same as in the previous section. (G.1) ensures a BH bifurcation at $\alpha = 0$, while (G.4) prevents a change of BF scenario near $\alpha = 0$. Close to $\alpha = 0$, $x = 0$ is an equilibrium of $f^{(1)}$. We write the eigenvalues of $f^{(1)}(0, \alpha)$ as $\lambda_{1,2}(\alpha) = \mu(\alpha) \pm i\omega(\alpha)$, with $\mu^0 = 0$ and $\omega^0 > 0$. We further assume the transversality and genericity of the Hopf bifurcation, i.e.,

(G.5) $\qquad \mu_\alpha^0 \neq 0 \quad$ and $\quad l_1^0 \neq 0$,

where l_1 is the first Lyapunov coefficient of the Hopf normal form (see, e.g., Kuznetsov (2004), Sect. 3.5). Finally, we assume that the BF and Hopf bifurcation curve intersect transversely at $\alpha = 0$ in the α-parameter plane:

(G.6) $\qquad \langle (H_\alpha^\perp)^0, \mu_\alpha^0 \rangle \neq 0$.

Under these conditions, the vector field $f^{(1)}$ can be reduced to Hopf normal form (through smooth and invertible changes of variables and parameters, and a time reparametrization). The Filippov system then becomes

$$\dot{y} = \begin{cases} \begin{bmatrix} \beta_2 & -1 \\ 1 & \beta_2 \end{bmatrix} y + l_1(\beta)\|y\|^2 y + O(\|y\|^4), & \text{in } S_1, \\ v(\beta) + O(\|y\|), & \text{in } S_2, \end{cases} \quad (5)$$

where $v(\beta)$ is the constant part of $f^{(2)}$, in the new variables and parameters. The parameters β can be chosen so that $\beta_2 = 0$ is the Hopf curve, while $\beta_1 = 0$ is the BF curve.

As mentioned in the Introduction, two simple Filippov systems have already been proposed to unfold the BH bifurcation (di Bernardo et al., 2008b; Guardia et al., 2009). In di Bernardo et al. (2008b), however, condition (G.4) is not satisfied, so that a *generalized boundary equilibrium* bifurcation (the change between persistence and nonsmooth-fold scenarios, see Della Rossa and Dercole (submitted)) concomitantly occurs. Indeed a fold bifurcation curve between pseudoequilibria emanates from the BH point tangentially to the BF curve (see Fig. 5 in di Bernardo et al. (2008b)). By contrast, the system in Guardia et al. (2009) is generic but cannot serve as a canonical system (i.e., a generic 2D Filippov system cannot be reduced to it by smooth coordinate transformations and time-reparametrization), since the Hopf normal form is assumed together with an horizontal discontinuity boundary.

Besides the BF and Hopf bifurcations, which intersect orthogonally, there are generically no other local bifurcations. By contrast there are two candidate global bifurcations: the first is a SH bifurcation occurring when the tangency point close to $y = 0$ is connected with the
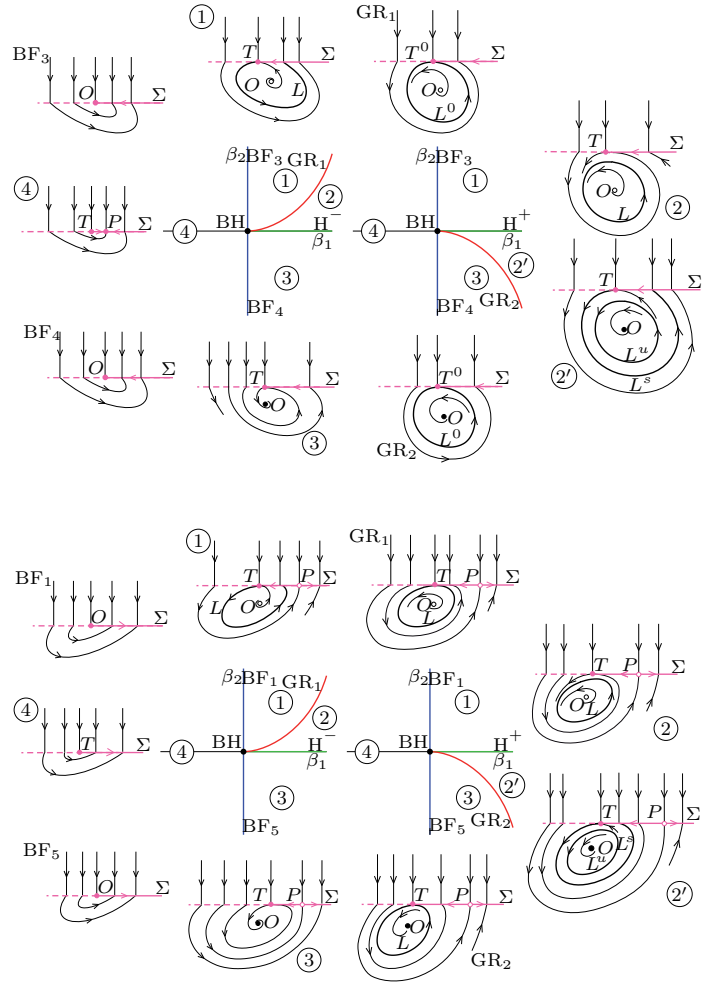

Fig. 4. BH universal local bifurcation diagrams. Top/bottom: persistence/nonsmooth-fold scenario; left/right: super-/sub-critical Hopf (tagged respectively H^- and H^+).

pseudo-saddle colliding with $y = 0$ at the BF; the second is the grazing (GR) of the limit cycle originating through the Hopf bifurcation. A SH can however be excluded, as the BF_1–BF_2 test-function introduced in section 2 does not vanish at a generic BH singularity.

As for the GR bifurcation, the cycle exists for $\beta_2 \gtrless 0$ (and is stable/unstable) if the Hopf is super-/sub-critical ($l_1^0 \lessgtr 0$ in (G.5)) and is geometrically a circle of radius $\sqrt{-\beta_2/l_1^0} + O(\beta_2)$ (where $O(\beta_2)$-terms are smooth functions of β_1).

Let $\sigma(\beta)$ be the distance of the equilibrium $y = 0$ from the boundary Σ, with positive/negative values if $H(0, \beta)$ is negative/positive, in order to make $\sigma(\beta)$ differentiable at $\beta = 0$. Thanks to (G.1) and (G.3), and to our choice of β_1, we can write σ as

$$\sigma(\beta) = \sigma_{\beta_1}^0 \beta_1 + O(\|\beta\|^2), \quad (6)$$

where $\sigma_{\beta_1}^0$ can be shown to be generically nonzero. Then, the asymptotic of the GR bifurcation curve (GR_1/GR_2 if $l_1^0 \lessgtr 0$ in (G.5)) is obtained by equating the radius of the cycle with the distance σ and by eliminating nonleading terms, i.e.,

$$\sqrt{-\beta_2/l_1^0} \simeq \sigma_{\beta_1}^0 \beta_1. \quad (7)$$

The GR curve hence emanates from $\beta = 0$ tangentially to the β_1-axis (the Hopf curve) with positive β_1 (the equilibrium $y = 0$ is admissible) and positive $-\beta_2/l_1^0$.

The bifurcation diagrams of the BH singularity locally to $\beta = 0$ are reported in Fig. 4. Generically, there are four cases, depending on whether the Hopf bifurcation is super- or sub-critical ($l_1^0 \lessgtr 0$ in (G.5), left/right panels in the figure) and on the BF scenario, persistence or nonsmooth-fold (positive/negative sign in (G.4), top/bottom; BF scenarios are defined in the caption of Fig. 2).

4. EXAMPLE: ON-OFF HARVESTING CONTROL OF A PREY-PREDATOR ECOSYSTEM

We have used the results presented above to analyse possible regulation strategies on a hunting reserve, modelled as a di-trophic food chain with harvesting of the predator. The model is a variant of the classical Rosenzweig-MacArthur prey-predator model. The densities of the prey and of the predator are the variables x_1 and x_2, and the predator population is harvested when abundant, i.e., when $x_2 > \alpha - px_1$. Parameter α is a safety threshold, while p models an additional decrease in the threshold when the prey is abundant. An abundant prey guarantees a faster predator recovery, so that harvesting is allowed at lower predator densities.

The system's equations where $x_2 < \alpha - px_1$ (in S_1) are

$$\dot{x}_1 = x_1(1 - x_1) - \frac{ax_1}{b + x_1}x_2, \tag{8a}$$

$$\dot{x}_2 = \frac{ax_1}{b + x_1}x_2 - dx_2. \tag{8b}$$

The prey grows logistically in the absence of predators and the predation rate follows the Holling type-II functional response—the Rosenzweig-MacArthur model—-see, e.g., Thieme (2003)). In S_2, where $x_2 > \alpha - px_1$, an extra mortality term $-Ex_2$ is added to (8b) due to harvesting. Parameter E measures the harvesting effort and can be controlled, e.g., by fixing the number of hunting licenses being released. Similar models, with $p = 0$, are discussed for example in Kuznetsov et al. (2003); Dercole et al. (2003).

Overall, parameters α, E, and p are determined by the harvesting policies and thus can be controlled by the legislator, whereas a, b, and d depend on biological factors and are typically not controllable. We have set the parameters to the values $p = 0.1$, $a = 0.3556$, $b = 0.15$, $d = 0.04444$, and studied the system in the plane (α, E), obtaining the diagram in Fig. 5. The bifurcation diagram that we have obtained (top-left panel) is rooted on two codimension-two points, a BH with nonsmooth fold scenario, and a HBF. In all the domain of the diagram there exist a large attracting limit cycle that is not affected by the depicted bifurcations. As show in the state portraits, the cycle lies partially below the threshold. This is an undesirable behaviour, since it implies that the prey becomes, periodically, dangerously scarce, and hunting must be prohibited for extended periods of time (see Fig. 6). However, in the shaded region of the bifurcation diagram in Fig. 5 there exist a second attractor: it is either a stable focus (in the dark grey region), or a stable limit cycle (in the light grey region). Both these attractors lie on or above the harvesting threshold, where
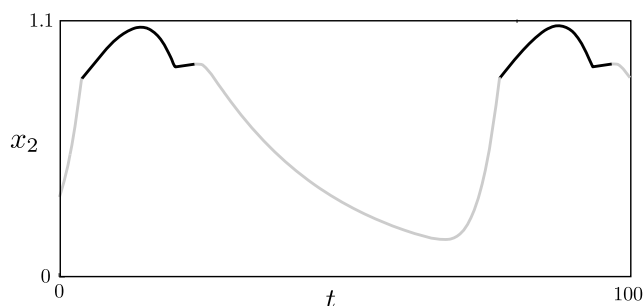

Fig. 6. The "bad" stable limit cycle of system (8), simulated at $E = 0.21$, $\alpha = 0.91$. The black part of the cycle lies above (or on) the harvesting threshold, the grey one below.

hunting is allowed, and thus are acceptable regimes. Notice that we have not detailed the physical meaning of the sliding behaviour. Mathematically speaking, sliding means that at each time the harvesting effort takes the value in $[0, E]$ that keeps the predator density at the harvesting threshold. Although this fine tuning of the effort is often hard to be implemented, it can be well approximated by high-frequency switching between fully open (effort E) and closed hunting (e.g., by allowing hunting only a few days per week).

Quite surprisingly, the "good" attractors are present for low values of α (i.e., less restrictive hunting regulation) and high values of E (i.e., more licences)! This suggests that a higher harvesting effort, which keeps the density of predators low, contributes to containing the system's oscillations by preventing the predator from consuming nearly all of its food source. The result is the creation of an attractor with smaller amplitude oscillations (the small cycle) or no oscillations at all (the stable focus). By suitably steering the system's orbits these attractors can be selected. These results are in contrast with most of the harvesting policies that can be imagined on an intuitive ground. For example, if the harvesting threshold is fixed by conservation ecologists and the system attains an equilibrium above but close to the threshold (see panel ① in Fig. 5), then one might think of increasing the predator density with a milder harvesting effort. By contrast, our results show that this might induce the destabilization of the equilibrium, leading to small oscillations, and eventually to the disappearance of the "good" attractor (see transitions ①–④).

To conclude, notice that the model above with $p = 0$, studied in Kuznetsov et al. (2003); Dercole et al. (2003), exhibits a degenerate BH bifurcation. This modifies the bifurcation diagram in Fig. 5, and adds a pseudo saddle-node curve that emerges from the BH point and is indeed visible in the bifurcation diagrams found in the above cited references.

REFERENCES

Astolfi, A. and Marconi, L. (2008). *Analysis and Design of Nonlinear Control Systems.* Springer-Verlag.

F. Della Rossa and F. Dercole. Generalized boundary equilibria in n-dimensional Filippov systems. *Physica D*, (submitted).
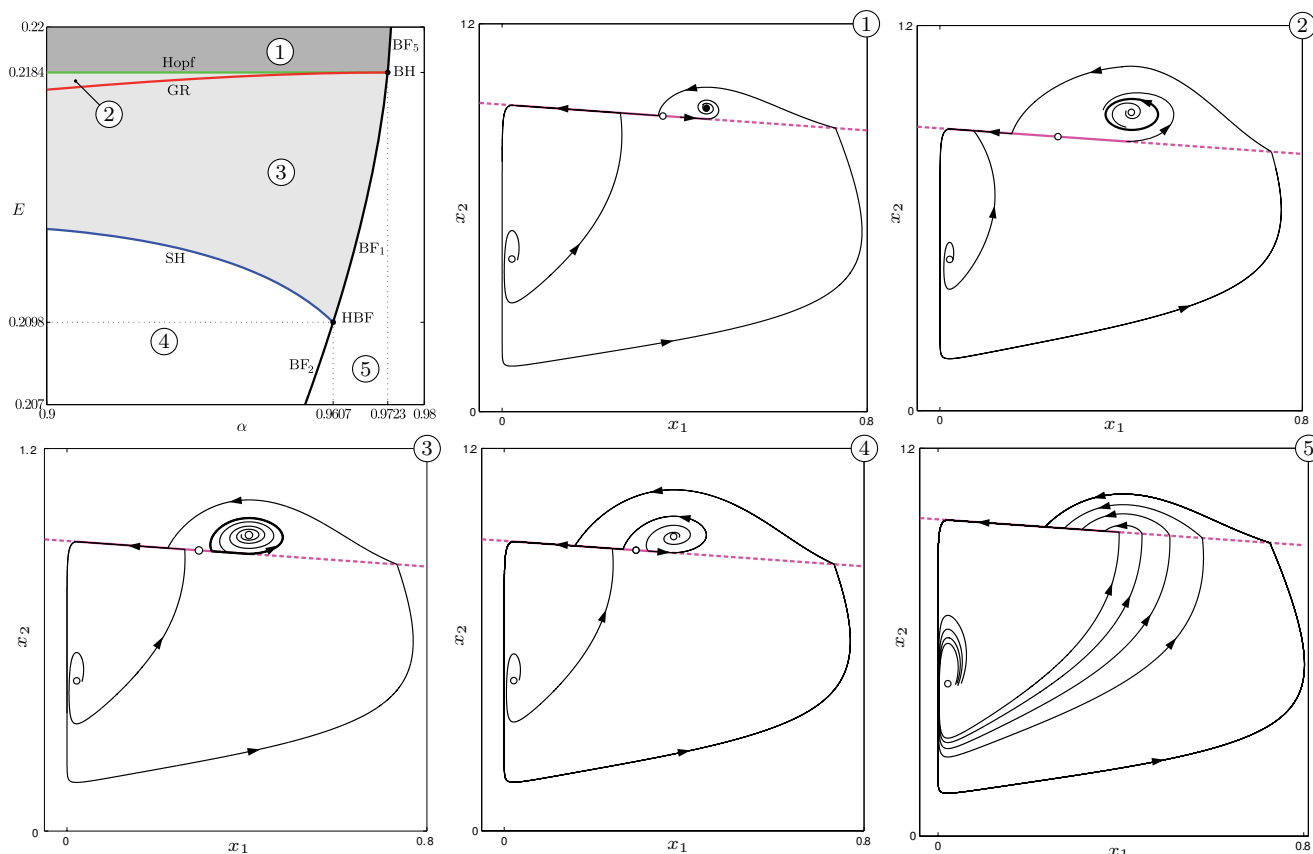
Fig. 5. Bifurcations of system (8). In the shaded area of the bifurcation diagram (top-left panel) there is an attractor lying entirely above the harvesting threshold: a limit cycle in the light grey area, a stable focus in the dark grey area. The other panels show an example of the state portrait in each region.

Colombo, A., di Bernardo, M., Hogan, S.J., and Jeffrey, M.R.. Bifurcations of piecewise smooth flows: Perspectives, methodologies and open problems. *Physica D*, (submitted).

Dercole, F., Della Rossa, F., Colombo, A., and Kuznetsov, Y.A. . Two degenerate boundary equilibrium bifurcations in planar Filippov systems. *SIAM J. Appl. Dyn. Syst.*, (submitted).

Dercole, F., Gragnani, A., Kuznetsov, Yu. A., and Rinaldi, S. (2003). Numerical sliding bifurcation analysis: An application to a relay control system. *IEEE Trans. Circuits-I*, 50, 1058–1063.

Dhooge, A., Govaerts, W., and Kuznetsov, Yu. A. (2002). MATCONT: A MATLAB package for numerical bifurcation analysis. *ACM Trans. Math. Software*, 29, 141–164.

di Bernardo, M., Budd, C.J., Champneys, A.R., and Kowalczyk, P. (2008a). *Piecewise-smooth Dynamical Systems: Theory and Applications.* Springer-Verlag.

di Bernardo, M., Pagano, D.J., and Ponce, E. (2008b). Nonhyperbolic boundary equilibrium bifurcations in planar Filippov systems: a case study approach. *Int. J. Bifurcat. Chaos*, 18, 1377–1392.

Doedel, E.J., Champneys, A.R., Dercole, F., Fairgrieve, T.F., Kuznetsov, Yu. A., Oldeman, B., Paffenroth, R.C., Sandstede, B., Wang, X.J., and Zhang, C.H. (2007). AUTO-07p: Continuation and bifurcation software for ordinary differential equations. Department of Computer Science, Concordia University, Montreal, QC.

Filippov, A.F. (1988). *Differential Equations with Discontinuous RHS*. Kluwer Academic Publishers, Dordrecht.

Guardia, M., Teixeira, M.A., and Seara, T. (2011). Generic bifurcations of low codimension of planar Filippov systems. *J. Differ. Equations*, 250, 1967–2023.

Krener, A.J., Kang, W., and Chang, D.E. (2004). Control bifurcations. *IEEE Trans. Autom. Control*, 49, 1231–1246.

Kuznetsov, Yu. A. (2004). *Elements of Applied Bifurcation Theory.* Springer-Verlag, Berlin, 3rd edition.

Kuznetsov, Yu. A. and Levitin, V.V. (1997). CONTENT: A multiplatform environment for analyzing dynamical systems. Dynamical Systems Laboratory, Centrum voor Wiskunde en Informatica, Amsterdam, The Netherlands available from `ftp.cwi.nl/pub/CONTENT`.

Kuznetsov, Yu. A., Rinaldi, S., and Gragnani, A. (2003). One parameter bifurcations in planar Filippov systems. *Int. J. Bifurcat. Chaos*, 13, 2157–2188.

Sieber, J., Gonzalez-Buelga, A., Neild, S.A., Wagg, D.J., and Krauskopf, B. (2008). Experimental continuation of periodic orbits through a fold. *Phys. Rev. Lett.*, 100, 244101.

Sieber, J., Krauskopf, B., Wagg, D., Neild, S., and Gonzalez-Buelga, A. (2009). Control-based continuation of unstable periodic orbits. *J. Comp. Nonlinear Dyn.*, 4, 331–340.

Thieme, H.R. (2003). *Mathematics in Population Biology.* Princeton University Press.